Structural Eng./Earthquake Eng., JSCE, Vol. 15, No. 1, 11s—18s, 1998 January
(J. Struct. Mech. Earthquake Eng., JSCE, No. 584/ I —42)

CRUSTAL STRUCTURE BENEATH THE AKASHI KAIKYO BRIDGE AS REVEALED BY EXPLOSION SEISMIC EXPERIMENTS

Kusnowidjaja MEGAWATI [1] and Hiromichi HIGASHIHARA [2]

[1] Member of JSCE, Ph.D., Earthquake Research Institute, the University of Tokyo
(1-1-1 Yayoi, Bunkyo-ku, Tokyo 113, Japan)
[2] Fellow of JSCE, Dr. Eng., Professor, Earthquake Research Institute, the University of Tokyo
(1-1-1 Yayoi, Bunkyo-ku, Tokyo 113, Japan)

A series of explosion seismic experiments were conducted along the *1995 Keihoku-Seidan Profile*. Most of the records acquired at the foundations of the Akashi Kaikyo Bridge had very poor S/N ratios. However, the *P*-waves of the explosions could be successfully detected after enhancing the records. The *P*-wave velocity structure was subsequently derived by fitting the travel times. The shallow crustal structure beneath the bridge is composed of four layers, with *P*-wave velocities ranging from 5.2 to 6.0 km/s. The structure derived here is an improvement to the shallow crustal structure revealed by previous explosion experiments done about thirty years ago.

Key Words: *explosion seismic experiment, the 1995 Keihoku-Seidan Profile, the Akashi Kaikyo Bridge, shallow crustal structure, P-wave velocity structure*

1. INTRODUCTION

The Hyogo-ken Nanbu Earthquake (M_{JMA} 7.2), occurred on January 17, 1995, causing severe damage in Kobe and Awaji Island, southwestern Japan. The hypocenter of the earthquake as released by the Japan Meteorological Agency[1] was at 34.607° N latitude and 135.043° E longitude with a depth of 14.3 km. The epicenter was located about two km east of the Akashi Kaikyo Bridge, which was under construction at the time. The earthquake caused large permanent horizontal and vertical displacements at the anchorages and piers of the bridge. The displacements were induced mainly by the deformation of the crust, without any significant slips between the bases of the foundations and the ground[2),3)].

The Research Group for Explosion Seismology (RGES) of Japan, founded in 1950, has continuously conducted explosion seismic observations in various regions of Japan[4),5)]. Since 1979, the Group has carried out these experiments under the Japanese Earthquake Prediction Program to gather basic data for earthquake prediction research. Detailed crustal structures have been revealed in many regions of Japan, such as the northern[6),7)] and central[8),9)] regions of Honshu Island, the Izu Peninsula[10)] and Nagano[11)]. However, the structure in the Kobe-Awaji region has not been sufficiently investigated.

Before the Hyogo-ken Nanbu Earthquake, a number of crustal investigations utilizing explosion seismic experiments had been conducted along profiles that crossed the Akashi Strait. The first one was a series of explosions done in Miboro, Gifu Prefecture from 1957 to 1960[12),13)]. Temporary observatory stations were aligned in three profiles in the central region of Honshu Island, with one of the profiles crossing the Akashi Strait. The Miboro explosion points were located approximately 230 km northeast of the Akashi Strait.

The second experiment was an explosion done in Toyama, Kochi Prefecture, Shikoku in December 1965[14),15)]. This explosion was intended to be the reverse shot of the Miboro explosions. Eighteen observatory stations were temporarily aligned in a profile, starting from Kochi to the north of the Biwa Lake, with intervals of 20 – 30 km. The Toyama explosion point was located about 170 km southwest of the Akashi Strait. With such long epicentral distances, the explosion waves recorded near the Akashi Strait during the two experiments are expected to have refracted or reflected from the

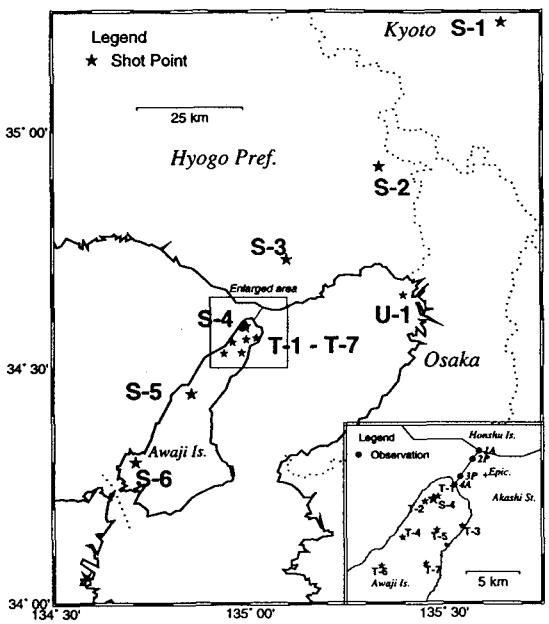

Fig.1 1995 Keihoku-Seidan explosion points.

basaltic layers of the crust or the upper mantle layers. Thus, the information of the shallow crustal structure beneath the strait revealed from these experiments was approximate.

In order to study the effects, behavior and characteristics of the seismic waves generated by the Hyogo-ken Nanbu Earthquake, more precise crustal structures in Kobe and Awaji Island are necessary. The objective of this study is to reveal the crustal structure beneath the Akashi Strait by utilizing a new series of explosion seismic data recorded at the foundations of the Akashi Kaikyo Bridge.

2. DESCRIPTION OF EXPLOSION EXPERIMENT

A new series of explosion seismic experiments were carried out along a profile, starting from Kyoto District to the southern region of Awaji Island. These experiments were conducted by the RGES from December 12 to 15, 1995. **Figure 1** shows the map of the profile that was named the *1995 Keihoku-Seidan Profile*. The stars indicate the shot points accompanied by the explosion codes. The length of the profile was about 140 km and a total of fourteen explosions were carried out during the three days of experiments. Two hundred and five observatory stations, not shown in the figure, were temporarily

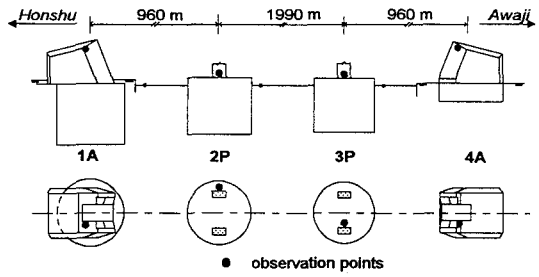

Fig.2 Locations of the observation points on the foundations

deployed along the profile. The inset shows a more detailed map of the northern tip of Awaji Island. The line with four solid circles indicates the Akashi Kaikyo Bridge and its four foundations (1A, 2P, 3P and 4A). A and P denote anchorage and pier, respectively. The cross mark shows the epicenter of the Hyogo-ken Nanbu Earthquake.

We, as an independent group from the RGES, took part in the experiments to record the explosion signals on the four foundations of the bridge. The locations of the observation points on the foundations are denoted by the solid circles in **Fig.2**.

The explosions were conducted by igniting dynamite buried inside boreholes. Each explosion event used one borehole, except events S-1 and S-6, in which two boreholes were used for each. The positions (latitude and longitude) of the shot points, date and exact time of the explosions, depth of the boreholes and weight of dynamite are given in **Table 1**.

Datamark LS-8000 units, manufactured by the *Hakusan Corp.*, were used for data recording. These compact recorders have internal clocks, which were adjusted twice before and twice again after each series of measurements, to synchronize the time of all recorders used in the experiment. The time calibrations were done through GPS receivers that were connected to all recorders. The timing accuracy in the present system was in the order of 0.1 milliseconds.

Geophones *L-22D* manufactured by *Mark Products, Inc.*, were used for the vertical components. The sensors were velocity-type seismographs with a natural frequency of 2.0 Hz and a damping factor of 0.7. Although the horizontal components were also recorded, the discussion in the present paper will be confined to the *P*-wave arrivals that can be sufficiently identified from the vertical components alone. Thus, the horizontal components will not be presented in this paper.

Table 1 General information of the explosion experiments.

Date of explosion	Explosion event	Position		Time of explosion	Depth of bore hole (m)	Weight of dynamite (kg)
		Latitude (N)	Longitude (E)			
Dec. 12, 1995	S-1	35°13'47"80	135°39'03"80	02:02:00.281	57	350
		35°13'47"60	135°39'04"10	02:02:00.281	57	350
	S-2	34°55'31"10	135°20'12"40	02:12:00.810	63	400
	S-3	34°43'45"00	135°05'55"30	02:22:00.439	57	350
	S-4	34°35'12"50	134°59'22"50	02:41:59.945	63	400
	S-5	34°26'41"50	134°51'02"40	02:52:00.444	57	350
	S-6	34°17'56"00	134°42'23"30	03:02:00.369	57	350
		34°17'54"80	134°42'23"30	03:02:00.369	57	350
Dec. 14, 1995	T-2	34°35'05"50	134°58'51"90	02:02:25.047	32	150
	T-4	34°33'15"90	134°57'27"00	02:12:10.271	32	150
	T-5	34°33'36"60	134°59'35"40	02:22:10.289	32	150
	T-7	34°31'55"40	134°58'53"10	02:32:10.407	32	150
	U-1	34°39'07"50	135°23'54"70	02:42:10.753	57	350
Dec. 15, 1995	T-1	34°35'20"90	134°59'40"00	02:02:11.623	32	150
	T-3	34°33'49"40	135°01'09"00	02:12:09.779	32	150
	T-6	34°31'49"60	134°56'08"30	02:22:10.448	32	150

3. DATA PROCESSING AND SIGNAL ENHANCEMENT

The vertical components recorded at 1A, 2P, 3P and 4A during explosion S-4 are shown in **Fig.3**, from top to bottom, respectively. The reference time (0.0 s) is the explosion time. The sampling frequency of the records was set at 200 Hz to avoid aliasing problems within the significant frequency ranges. The first arrivals of the *P*-waves, denoted by P in the figure, can be detected clearly in the four records due to the large explosive charge and short epicentral distances. The *SV*-waves are also detected in the records at 1A and 2P.

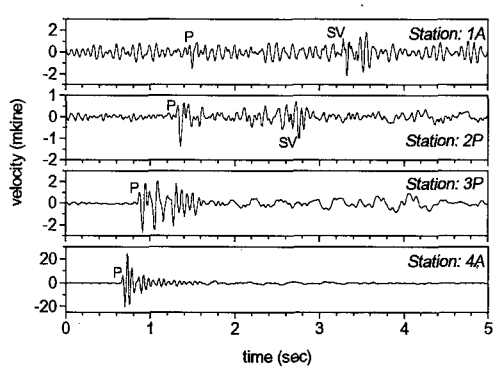

Fig.3 Vertical components recorded during the explosion S-4.

Out of the fourteen explosions done during the experiments, only explosion signals from three events, namely S-4, T-1 and T-3, can be clearly detected in the raw records. The data recorded during the other explosions have very poor signal to noise (S/N) ratio. These records have to be enhanced in order to detect the arrivals of the explosion waves.

To enhance the records, it is necessary to separate the signals generated by the explosions from the noise. The predominant frequency ranges of the *P*-waves are identified by examining the Fourier spectra of the records that show clear explosion signals, i.e. S-4, T-1 and T-3, within the time windows of the waves. **Figure 4** shows the spectra of the record at 4A during explosion S-4 (bottom trace of **Fig.3**). Two time windows are considered: the first one, which contains the explosion signals, is from 0.0 to 5.12 s, while the second window, which is expected to contain noise only, starts one minute after the explosion and lasts 5.12 s. In this figure, the predominant frequencies of the *P*-wave are identified in the range of 14 – 22 Hz. On the other hand, the noise has wide-band frequencies ranging from 6 to 14 Hz. Thus, the *P*-wave and noise show distinct frequency bands.

Figure 5 (top) shows the vertical component recorded at 4A during explosion T-7. Time 0.0 s refer to the time of the explosion. The distance between the station and the explosion point was 7.904 km, so it may be estimated that the explosion signals would arrive at the station about two seconds after the explosion. As can be seen in this figure, no clear explosion signal can be observed due to poor S/N ratio. **Figure 5** (bottom) shows the same record after being band-pass filtered with passing range from 14 to 22 Hz. The butterworth filter was used. The filtering was applied forward and backward over

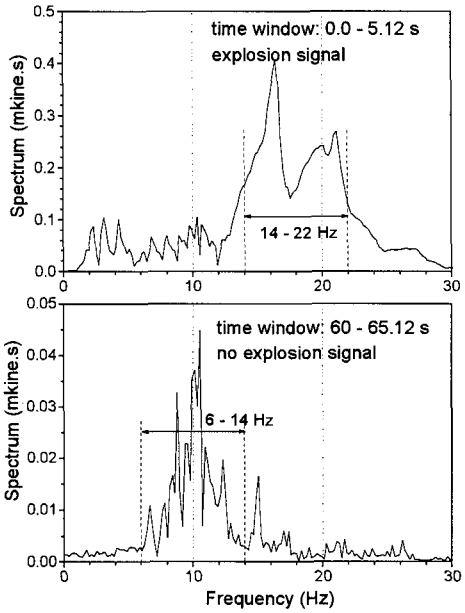

Fig.4 Spectra of record at 4A during explosion S-4.

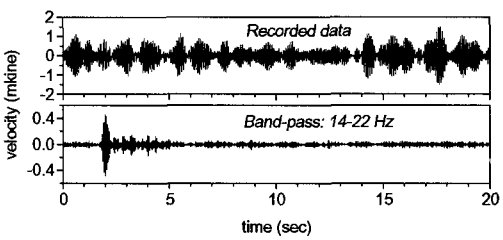

Fig.5 Vertical component recorded at 4A during the explosion T-7.

the data to obtain zero-phase result. The filtered record shows a clear arrival of the *P*-wave two seconds after the explosion.

After band-pass filtering all records, the first arrival can be detected in almost all of them. The signals generated by explosions S-1 and S-2, located more than 40 km northeast of the bridge, were too weak to be enhanced. The explosion signal S-5 could not be successfully enhanced due to the long epicentral distance and medium charge size.

4. *P*-WAVE VELOCITY STRUCTURE

(1) *P*-wave travel-time curve

The travel-time curves of the *P*-waves from explosions S-4, T-1 and T-2, which were located closest to the bridge are shown in **Fig.6**. All the sources were located south of the bridge, thus the

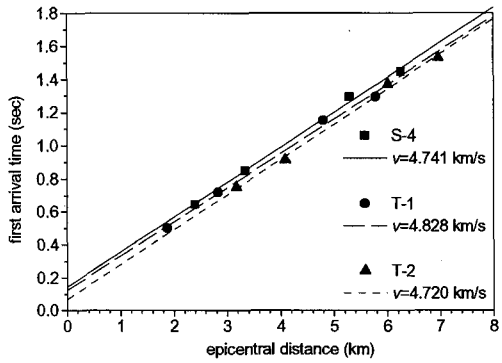

Fig.6 Travel-time curves of the *P*-waves from shot points S-4, T-1 and T-2.

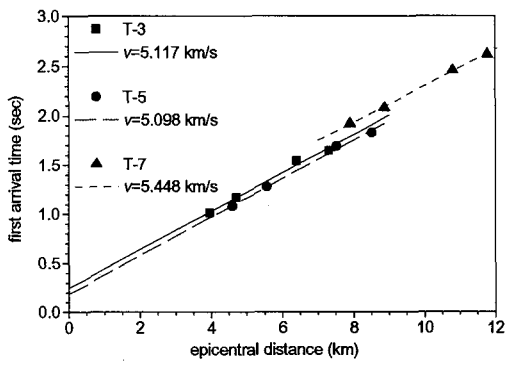

Fig.7 Travel-time curves of the *P*-waves from shot points T-3, T-5 and T-7.

P-waves arrived at 4A (southern anchorage) first and propagated subsequently to the north. The linear regression lines for the three events are also shown in the figure. The apparent velocities of the *P*-waves from these events, which correspond to the slope of the regression lines, show similar values. These waves may be assumed to have propagated through the same layer that has the same velocity. The apparent velocity, however, does not indicate the head wave velocity because the former is influenced by the dipping of the layer[16].

Figure 7 shows the *P*-wave travel-time curves for explosions T-3, T-5 and T-7. The shot points of T-3 and T-5 were located about 4 km south of 4A, while the shot point of T-7 was about 8 km away. The apparent velocities of the *P*-waves from T-3 and T-5 are in the order of 5.1 km/s, and that from T-7 is 5.448 km/s. These velocities are higher than those of the previous three events (S-4, T-1 and T-2). These results suggest that the apparent velocity increases with the increase of the epicentral distance. This is reasonable because the *P*-waves originate from sources located farther away may propagate through

deeper layers that are generally harder and have higher velocities. Thus, the *P*-waves from T-3 and T-5 are assumed to propagate through the same deeper layer, and that from T-7 propagated through yet deeper layer.

The *P*-wave from explosion S-6, which was located 43.5 km southwest of 4A shows an apparent velocity of 5.897 km/s. Thus, it is consistent with the above findings.

The records for T-4 could not be enhanced successfully, so they were excluded from the analysis. The *P*-waves from T-6 showed a very low apparent velocity of 4.735 km/s. This may be due to local characteristics of the crust in the vicinity of the shot point that cannot be explained by analyzing the records at the four foundations only.

(2) *P*-wave travel path model

Figure 8 shows the ray paths of the *P*-waves that propagate in a crustal structure with dipping interface between the sediment layer and the first crustal layer. Ray 1 denotes the ray path of the *P*-waves that originated from the very near sources, i.e. S-4, T-1 and T-2. The travel-time equation of Ray 1 that propagates along the interface of the sediment layer and Layer 1 is formulated as[16],

$$t = \frac{1}{v_{sd}}\left\{2h_{sd}^{(s)}\cos i_{c1}\cos\theta + x\sin(i_{c1}-\theta)\right\} \quad (1)$$

where t is the travel time, x is the epicentral distance, $h_{sd}^{(s)}$ is the thickness of the sediment layer beneath the explosion source, θ is the dipping angle of the interface, and i_{c1} is the critical angle of Ray 1, that is governed by Snell's Law as,

$$p_1 = \frac{\sin i_{c1}}{v_{sd}} = \frac{1}{v_1}. \quad (2)$$

Here p_1 is the horizontal slowness of Ray 1, which is constant for the entire travel path of the ray, and v_{sd} and v_1 are the *P*-wave velocities in the sediment layer and Layer 1, respectively.

As has been shown in the above section, *P*-waves that originated from the explosion sources located farther away, i.e. T-3, T-5, T-7 and S-6, propagated through the deeper layers of the crust. The second, third and forth crustal layers underlay the first layer, with the interfaces adjusted parallel to the above interface. This is a simple shallow crustal model adopted in this study because the complete records along the explosion profiles in the northern tip of

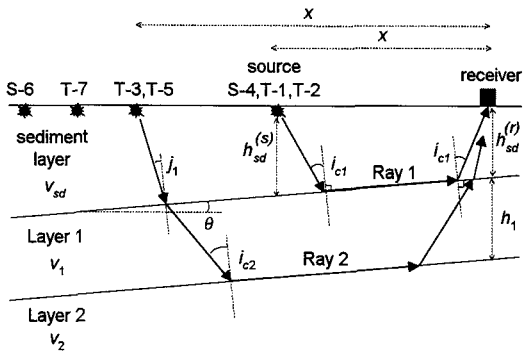

Fig.8 The ray paths of *P*-waves propagate in a crustal structure with dipping interface.

Awaji Island have not yet been made available. This model is applicable in the present study because the epicentral distances of the shot points used in the analysis were mainly confined within 10 km. The shallow crustal structure may not differ abruptly within such a short distance.

The travel-time equation of Ray 2, propagating through the interface of Layers 1 and 2, can be simplified by assuming a small dipping angle θ as,

$$t = \frac{\cos\theta}{v_{sd}\cos j_1}\left\{h_{sd}^{(s)} + h_{sd}^{(r)}\right\} + p_2\left\{\frac{x}{\cos\theta} - h_{sd}^{(s)}\frac{\sin(j_1+\theta)}{\cos j_1} - h_{sd}^{(r)}\frac{\sin(j_1-\theta)}{\cos j_1}\right\} + 2h_1\eta_1 \quad (3)$$

where j_1 and h_1 are the angle of incidence of the ray on Layer 1 and the thickness of the layer, respectively, $h_{sd}^{(r)}$ is the thickness of the sediment layer beneath the observatory station, p_2 is the horizontal slowness of Ray 2 and η_1 is a ray constant for Layer 1:

$$p_2 = \frac{\sin j_1}{v_{sd}} = \frac{\sin i_{c2}}{v_1} = \frac{1}{v_2} \quad (4)$$

$$\eta_1 = \frac{1}{v_1}\sqrt{1 - v_1^2 p_2^2} \quad (5)$$

The first term on the right-hand side of Eq. (3) is the travel-time of the down-going and up-coming parts of Ray 2 in the sediment layer. The second and third terms are the travel-time of the ray in Layer 1 and at the interface between Layers 1 and 2, which together are the travel-time equation for a single-horizontal-layer medium. Thus, the travel-time equations for rays propagating through the deeper

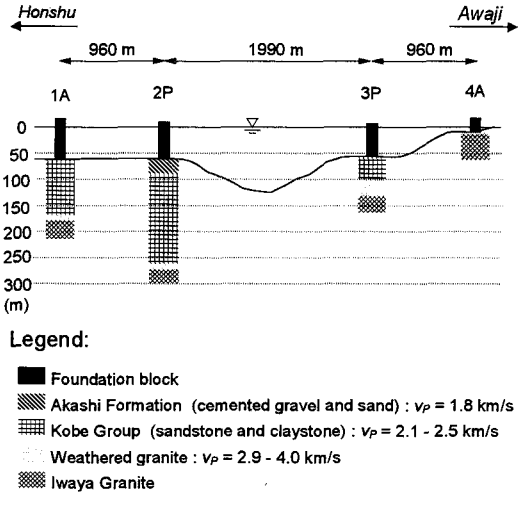

Fig.9 Soil profile under the foundations of the bridge obtained from the borehole investigations.

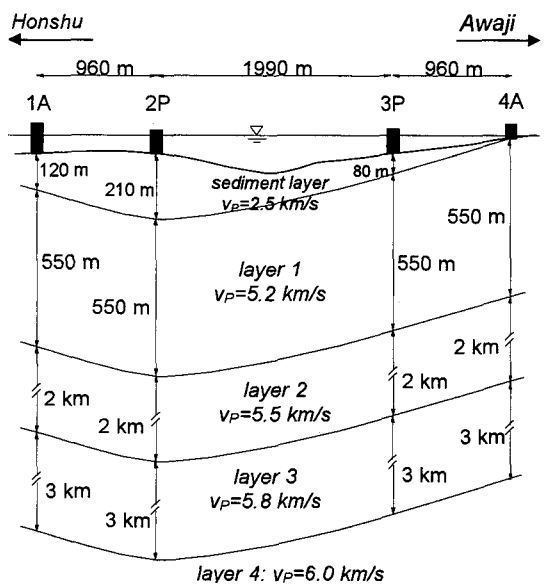

Fig.10 The sedimentary and crustal structure under the bridge as revealed from the present explosion experiments.

layers can be formulated by modifying the last two terms to the travel time for multi-horizontal-layer medium.

(3) *P*-wave velocity profile

Prior to the construction of the bridge, many boreholes for soil investigations were made in the construction site. The boreholes were made down to the depth of the granitic layers. The results of the soil investigations[17),18)], as shown in **Fig.9**, indicate that 4A is located directly on a granitic layer and the other foundations are located on sedimentary layers. 2P is located on the Akashi Formation which is composed of cemented gravel and sand. The *P*-wave velocity v_P and thickness of the layer are 1.8 km/s and 30 m, respectively. 1A and 3P are located on the Kobe Group which is composed of sandstone and claystone, with v_P ranging from 2.1 to 2.5 km/s. Beneath the Kobe Group, a weathered granite layer, with v_P of 2.9 – 4.0 km/s is found before the Iwaya granite.

The sedimentary structure can be simplified by considering the Akashi Formation, Kobe Group and weathered granite layers to be a single layer with an averaged v_P of 2.5 km/s. The thicknesses of the layer beneath 1A, 2P and 3P are 120 m, 210 m and 80 m, respectively. Since the thickness and velocity of the sedimentary layers beneath the foundations are known, the *P*-wave velocity of Layer 1, v_1, can be calculated by Eq. (1) to fit the travel-time curves shown in **Fig.6**. By trial and error, a value of 5.2 km/s that gives the best fit is obtained.

The thickness of Layer 1 and the velocity of Layer 2 are determined from the travel-time data of T-3 and T-5 by using Eq. (3). The thickness and velocities of the deeper layers are obtained from the travel-time data of T-7 and S-6. The crustal profile beneath the bridge as revealed from the present explosion experiments is shown in **Fig.10**. The velocity values shown in the figure are the *P*-wave velocities of the corresponding layers.

5. DISCUSSION

(1) Justification of the previous observations

Figure 11 shows the crustal structure along the Miboro-Toyama profile as revealed from the 1957-1960 Miboro explosions and 1965 Toyama explosion[15)]. The profile was a two-side explosion profile, thus the dipping of the deeper layers may be reasonably considered. Judging from the travel-time curves, the first and second arrivals of the explosion signals recorded in the vicinity of the Akashi Strait originated from the refractions of the upper mantle layers and the basaltic layers of the crust, respectively. The v_P of the basaltic and upper mantle layers derived from these experiments are 6.6 and 7.8 km/s, respectively. Although no reliable information was available for the shallow crustal structure beneath the Akashi Strait, the structure of the deep crust revealed from these explosions is quite reasonable.

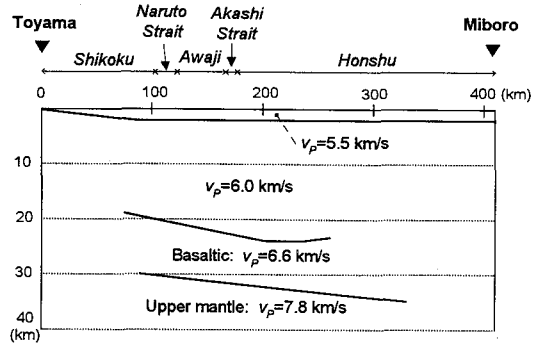

Fig.11 The crustal structure along the Miboro-Toyama profile.

Figure 12 shows the complete crustal structure beneath the Akashi Kaikyo Bridge after considering the data of the boreholes and the two previous explosions. The Akashi Formation layer with a v_P of 1.8 km/s is put beneath 2P. The basaltic and upper mantle layers underlay the granitic layers, and their thickness are recalculated from the travel-time data by considering the upper crustal structures revealed from the present observations.

(2) Geology

The geology of the sea-floor beneath the Akashi Kaikyo Bridge is composed of thin alluvium layers, the Akashi Formation of the Osaka Group, the Kobe Group and the Iwaya Granite[19),20)]. The alluvium layers mainly exist around the coast lines near Maiko (Honshu Island) and Nagahama (Awaji Island). The Akashi Formation is found near 2P, and the Kobe Group and Iwaya Granite outcrop around the center of the bridge and 4A, respectively.

The northern tip of Awaji Island is mainly composed of granitic rocks. The Nojima Granodiorite is most widely exposed in this area and is intruded upon by the Iwaya Granite in the northern margin. The Iwaya Granite where 4A is located is from the Mesozoic Period and its *P*-wave velocity, as found in the present investigations, is around 5.2 – 5.5 km/s. This layer is the superficial granitic layer found beneath the strait.

The Kobe Group, where 1A and 3P are located, dates from the early to middle Miocene Period and has a v_P of 2.5 km/s. The Akashi Formation is the early Pleistocene deposit with a quite low v_P of 1.8 km/s.

6. CONCLUSION

In the seismic response analysis of the Akashi Kaikyo Bridge, the crustal information beneath the bridge is very significant. The elastic properties of the crust govern the propagation characteristics of the seismic waves. The present research attempts to reveal the shallow crustal structure beneath the bridge by utilizing explosion seismic data.

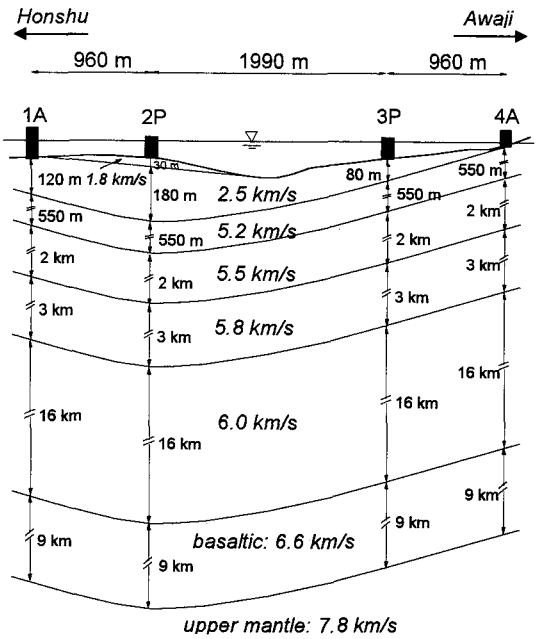

Fig.12 The complete crustal structure under the Akashi Kaikyo Bridge after justifications.

The *1995 Keihoku-Seidan* explosions provide sufficient data to reveal the detailed shallow crustal structure beneath the bridge. The profile of the sediment layers obtained from the explosion observations is in substantial agreement with those from the borehole data. This may be partly due to the very precise timing system in the present observations.

The first and second granitic layers obtained from the explosion experiments are identified as the Iwaya Granite of the Mesozoic Period that outcrop at the northern region of Awaji Island. The v_P of these layers is calculated as about 5.2 – 5.5 km/s. The sediment layers beneath the Akashi Strait are mainly composed of the Kobe Group and the Akashi Formation of the Osaka Group.

The shallow crustal structure beneath the strait is composed of four layers, with *P*-wave velocities ranging from 5.2 to 6.0 km/s. The structure derived here is an improvement to the shallow crustal structure revealed by the Miboro and Toyama explosion experiments done about thirty years ago.

ACKNOWLEDGMENT: The authors are indebted to the Honshu Shikoku Bridge Authority for

their helpful support and to the companies engaged in the construction of the Akashi Kaikyo Bridge for their cooperation during the observation. The authors wish to express sincere gratitude to the RGES, especially to Assoc. Prof. Takaya Iwasaki for invaluable discussions and for providing the digitized data of the map in **Fig.1**. The authors wish to thank Prof. Fumio Tatsuoka of the Department of Civil Engineering, the University of Tokyo for providing the borehole data. Thank is extended to Mr. John R. Rabone, ESP instructor, for reviewing the English grammar of this paper.

REFERENCES

1) Japan Meteorological Agency: The 1995 Hyogo-ken Nanbu Earthquake and its aftershocks, *Report Coord. Comm. Earthq. Pred.*, No. 54, 1995. (in Japanese)
2) Honshu Shikoku Bridge Authority: Investigation report of the influence of the Hyogo-ken Nanbu Earthquake to the Akashi Kaikyo Bridge, *Report of Honshu Shikoku Bridge Authority*, August 1995. (in Japanese)
3) Yamagata, M., Yasuda, M., Nitta, A., and Yamamoto, S.: Effects on the Akashi Kaikyo Bridge, Special Issue of *Soils and Foundations* on Geotechnical Aspects of the January 17 1995 Hyogoken-Nambu Earthquake, Japanese Geotechnical Society, pp. 179-187, 1996.
4) Research Group for Explosion Seismology: Explosion seismological research in Japan, *The Earth beneath the Continents*, ed. by Steinhart, J. S. and Smith, T. J., American Geophysical Union, Geophysical Monograph, Series 10, pp. 334-348, 1966.
5) Yoshii, T.: Crustal structure of the Japanese islands revealed by explosion seismic observations, *Zisin*, Vol. 46, No. 2, pp. 479-491, 1994. (in Japanese)
6) Asano, S., Okada, H., Yoshii, T., Yamamoto, K., Hasegawa, T., Ito, K., Suzuki, S., Ikami, A., and Hamada, K.: Crust and upper mantle structure beneath northeastern Honshu, Japan, as derived from explosion seismic observations, *J. Phys. Earth*, Vol. 27, Suppl., pp. S1-S13, 1979.
7) Iwasaki, T., Yoshii, T., Moriya, T., Kobayashi, A., Nishiwaki, M., Tsutsui, T., Iidaka, T., Ikami, A., and Masuda T.: Seismic refraction study in the Kitakami Region, northern Honshu, Japan, *J. Phys. Earth*, Vol. 41, pp. 165-188, 1993.
8) Sasatani, T., Yoshii, T., Ikami, A., Tanada, T., Nishiki, T., and Kato, S.: Upper crustal structure under the central part of Japan: Miyota-Shikishima Profile, *Bull. Earthq. Res. Inst., Univ. Tokyo*, Vol. 65, pp. 33-48, 1990.
9) Matsu'ura, R. S., Yoshii, T., Moriya, T., Miyamachi, H., Sasaki, Y., Ikami, A., and Ishida, M.: Crustal structure of a seismic-refraction profile across the Median and Akaishi Tectonic Lines, central Japan, *Bull. Earthq. Res. Inst., Univ. Tokyo*, Vol. 66, pp. 497-516, 1991.
10) Yoshii, T., Asano, S., Kubota, S., Sasaki, Y., Okada, H., Masuda, T., Murakami, H.,Suzuki, S., Moriya, T., Nishide, N., and Inatani, H.: Detailed crustal structure in the Izu Peninsula as revealed by explosion seismic experiments, *J. Phys. Earth*, Vol. 34, Suppl., pp. S241-S248, 1986.
11) Ikami, A., Yoshii, T., Kubota, S., Sasaki, Y., Hasemi, A., Moriya, T., Miyamachi, H., Matsu'ura, R. S., and Wada, K.: A seismic-refraction profile in and around Nagano Prefecture, central Japan, *J. Phys. Earth*, Vol. 34, pp. 457-474, 1986.
12) Research Group for Explosion Seismology: Crustal structure in central Japan as derived from the Miboro explosion-seismic observations. Part 1 explosions and seismic observations, *Bull. Earthq. Res. Inst., Univ. Tokyo*, Vol. 39, pp. 285-326, 1961.
13) Mikumo, T., Otsuka, M., Utsu, T., Terashima, T., and Okada, A.: Crustal structure in central Japan as derived from the Miboro explosion-seismic observations. Part 2 on the crustal structure, *Bull. Earthq. Res. Inst., Univ. Tokyo*, Vol. 39, pp. 327-349, 1961.
14) Research Group for Explosion Seismology: Observation of seismic waves from the Toyama explosion in Sikoku, Japan, *Zisin*, Vol. 27, No. 2, pp. 95-103, 1974. (in Japanese)
15) Aoki, H., and Muramatu, I.: Crustal structure in the profile across Kinki and Shikoku, Japan, as derived from the Miboro and the Toyama explosions, *Zisin*, Vol. 27, No. 2, pp. 104-109, 1974. (in Japanese)
16) Lay, T., and Wallace, T. C.: *Modern Global Seismology*, Academic Press, Inc., Chap. 3, 1995.
17) JSCE.: *Research Report on Earthquake Resistance of Foundations of the Honshu-Shikoku Bridge*, March 1988 (in Japanese).
18) JSCE.: Proposal of design outline of the Akashi Kaikyo Bridge, *Research Report on Earthquake Resistance of Foundations of the Honshu-Shikoku Bridge*, March 1988 (in Japanese).
19) Huzita, K., and Maeda, Y.: *Geology of the Suma District*, Geology Survey of Japan, 1984. (in Japanese with English abstract)
20) Mizuno, K., Hattori, H., Sangawa, A., and Takahashi, Y.: *Geology of the Akashi District*, Geology Survey of Japan, 1990. (in Japanese with English abstract)

(Received August 13, 1996)

爆破による人工地震実験によって明らかにされた明石海峡大橋直下の地質構造

Kusnowidjaja MEGAWATI ・東原紘道

1995年に京都北部—淡路島西部断面に沿って，一連の爆破実験がおこなわれた．明石海峡大橋の基礎部での観測記録はS/N比が乏しいものであったが，波形処理により，爆破震源からのS波を求めることができた．そして，到達時刻のフィッティングで地下のP波速度構造を求めた．明石海峡大橋直下の地下構造はP波速度5.2 - 6.0 km/sの４つの層から構成されていることがわかった．本研究で明らかになった地下構造は，およそ30年前の爆破実験で求められた地下構造に較べ，浅部をより詳細に記述するものとなった．